HHS Public Access

Author manuscript

Cell Tissue Res. Author manuscript; available in PMC 2022 May 01.

Published in final edited form as:

Cell Tissue Res. 2021 May ; 384(2): 367–387. doi:10.1007/s00441-020-03379-3.

Characterization of the structure, vascularity, and stem/progenitor cell populations in porcine achilles tendon (PAT)

Jianying Zhang[1], **Feng Li**[1], **Kelly M. Williamson**[1], **Susheng Tan**[2], **Devon Scott**[1], **Kentaro Onishi**[3], **MaCalus V. Hogan**[1], **James H-C. Wang**[1,*]

[1]MechanoBiology Laboratory, Department of Orthopaedic Surgery, University of Pittsburgh School of Medicine, 210 Lothrop St., BST, E1640, Pittsburgh, PA 15213, USA

[2]Department of Electrical and Computer Engineering, University of Pittsburgh, Pittsburgh, PA 15213, USA

[3]Department of Physical Medicine and Rehabilitation, University of Pittsburgh, Pittsburgh, PA, 15213, USA

Abstract

This study aimed to characterize porcine Achilles tendon (PAT) in terms of its structural components, vascularity, and resident tendon cells. We found that PAT is composed of a paratenon sheath, a core of fascicles, and an endotenon/interfascicular matrix (IFM) that encases the fascicle bundles. We analyzed each of these three tendon components structurally using tissue sections, and by isolating cells from each component and analyzing *in vitro*. Many blood vessel-like tissues were present in the paratenon and IFM but not in fascicles, and the vessels in the paratenon and IFM appeared to be inter-connected. Cells isolated from the paratenon and IFM displayed characteristics of vascular stem/progenitor cells expressing the markers CD105, CD31, with α-smooth muscle actin (α-SMA) localized surrounding blood vessels. The isolated cells from paratenon and IFM also harbored abundant stem/progenitor cells as evidenced by their ability to form colonies, and express stem cell markers including CD73 and CD146. Furthermore, we demonstrate that both paratenon and IFM isolated cells are capable of undergoing multi-differentiation. In addition, both paratenon and IFM cells expressed elastin, osteocalcin, tubulin polymerization promoting protein (TPPP), and collagen IV, whereas fascicle cells expressed none of these markers, except collagen I. The neurotransmitter substance P (SP) was also found in the paratenon and IFM localized surrounding blood vessels. The findings of this study will help us to better understand the vascular and cellular mechanisms of tendon homeostasis, injury, healing, and regeneration.

[*]**Corresponding author:** wanghc@pitt.edu.

Conflicts of interest

On behalf of all authors, the corresponding author states that there is no conflict of interest in this study.

Compliance with ethical statements

Ethical approval

This article does not contain any studies with human participants or animals performed by any of the authors.

Keywords

Achilles tendon; paratenon; interfascicular matrix; fascicles; stem cells

Introduction

Tendons are specialized connective tissues that enable joint movement by transmitting mechanical forces from muscle to bone. The Achilles tendons (AT) of humans and large animals have a well-defined structure that consists of three main components: a paratenon sheath surrounds bundles of collagen fascicles, with individual fascicles separated by an endotenon or interfascicular matrix (IFM) (Benjamin et al. 2008; Kannus 2000; Kapetanakis et al. 2017). Fascicles are the fundamental functional units of tendon, and are comprised of tightly packed parallel collagen fibers and fibroblast-like cells, while IFM and paratenon are composed of loose membrane-like structures with the presence of blood vessels and a likely diverse cell population. While each of the three compartments has specialized structures for the overall function of tendon, the role of each in performing specific functions in tendon maintenance, injury, and healing are not well understood. Tendon is constantly subjected to excessive mechanical loading and overuse; hence tendon is very prone to injuries that are both acute and chronic. Although Achilles tendon is the largest and strongest tendon in the body, it is commonly injured (Maffulli et al. 2004), which is generally attributed to poor vascularity in human Achilles tendon (Ahmed et al. 1998; Theobald et al. 2005). Traditionally, tendon subcomponents exhibit variable levels of vascularity, with fascicles as a largely avascular structure surrounded by vascularized IFM and paratenon, leading to an overly generalized description of tendon as hypovascular (Fenwick et al. 2002; Tempfer and Traweger 2015).

Like other connective tissues, human and animal tendons harbor tendon stem/progenitor cells (TSCs) (Bi et al. 2007; Rui et al. 2010; Zhang and Wang 2010). Moreover, sophisticated lineage tracing efforts and single cell RNA technology (Dyment et al. 2014; Yin et al. 2016) have been applied to identify distinct subpopulations of these cells. However, these advances still lack progress in analyzing the location of subpopulations within these three components of tendon (*i.e.* paratenon, IFM, and fascicles), and the differential morphological and functional characteristics of these subpopulations and tissues have not been thoroughly characterized yet. Lineage tracing techniques mostly rely on cell markers that are not specific to TSCs, and single cell analysis requires either a pooled collection of multiple tendons to produce results or culturing and expansion of tendon cells prior to analysis (Dyment et al. 2014; Yin et al. 2016). TSC isolation regularly involves the digestion of entire tendons rather than specific components, with at most the separation of the tendon sheath, or paratenon, from the tendon proper (Bi et al. 2007; Mienaltowski et al. 2013; Rui et al. 2010; Tan et al. 2013; Zhang and Wang 2010). Thus, such procedures may have inadvertently included IFM either in fascicles or paratenon, which may have affected the location-specific identification and analysis of specific cell populations. Further limitations exist in performing analysis of subpopulations of TSCs, such as size of the research animal and hence tendon, as well as the rarity of the cell.

It is possible that each individual component within tendon contains specialized and unique stem cells whose role is to repair their own individual structural component in the event of injury (Nichols et al. 2019; Snedeker and Foolen 2017). In order to understand how injured tendon accomplishes healing and repair, it is important to understand the relationship between tendon structure, vascularity, and resident cells, and how each contributes to tendon function and healing. Therefore, the aim of this study was to perform a detailed characterization and comparison of three well-defined components in terms of their structural and cellular properties using scanning electron microscopy (SEM), as well as immunohistochemical and cytochemical analyses with specific markers. For this purpose, we chose easily available juvenile porcine Achilles tendon, considering its large size and the difficulty in obtaining normal human tendon tissues. We dissected each of the three main tendon components namely paratenon, IFM, and fascicles separately (Benjamin et al. 2008; Kannus 2000; Kapetanakis et al. 2017), and characterized them in regard to their differential structural features, vascularity, and resident cellular populations. Our results show distinct structural features for each component with a clear separation between them, and a clear vascularity through the presence of blood vessels extending from the paratenon into the IFM but are not present in fascicles. The vascularity of paratenon and IFM is supported by the presence of a specific population of vascular stem cells with differential properties within both of them, but this vascularity is not evident in fascicles.

Materials and methods

Tissue samples and histochemical staining on PAT sections

The hind legs of a 6-month old juvenile male domesticated pig were obtained from Thoma meat market (Saxonburg, PA), from which two fresh Achilles tendons were removed, imaged, and each component (paratenon, fascicles, IFM) was carefully dissected under sterile conditions as described elsewhere (Benjamin et al. 2008; Kapetanakis et al. 2017). For dissection, the paratenon was separated from the epitenon and the paratenon was further analyzed separately. The epitenon remained with the tendon proper. Next, the IFM, or endotenon, was dissected separately from the epitenon. Collected tendon tissues were used within 24 hrs of slaughter. Harvested tissue samples focused specifically on midportion Achilles tendon. Tendon tissues were fixed with 4% paraformaldehyde at room temperature for 5 hrs, embedded in paraffin, and cut into longitudinal and cross sections with a thickness of 5 μm. To visualize tendon tissue structures, sections were stained either with hematoxylin and eosin (H&E) or with Safranin O and Fast Green (S&F) according to the standard protocols, and stained tendon sections were examined under light microscopy (Nikon eclipse, TE2000-U). Safranin O stains proteoglycans whereas Fast Green stains collagens.

Scanning electron microscopy (SEM) of PAT sections

Achilles tendon samples were fixed with 3% glutaraldehyde for 30 min, and then washed with PBS three times for 5 min/each. Fixed samples were then treated with a series of ethanol concentrations in distilled water for 15 min/each (10%, 30%, 50%, 60%, 70%, 80%, 90%, and 100% ethanol) for dehydration. The dehydrated tendon tissue samples were dried via the critical point drying process by liquid nitrogen. The dried tendon samples were

sputter coated with gold/palladium and examined under a JEOL SEM (Tokyo, Japan) with an accelerating voltage of 5.0 kV.

Immunostaining on PAT tissue sections

Fixed Achilles tendon tissue samples were mounted in OCT embedding compound and frozen at −80°C. The tissue block was cut into longitudinal and cross sections with 5 μm thickness by a cryostat. The tissue sections were incubated with the following antibodies separately: mouse anti-CD146 (1:500, Bio-RAD, Cat. MCA2141), mouse anti-CD105 (1:500, Abcam, Cat. ab69772, Cambridge, MA), mouse anti-collagen type I (1:500, Abcam, Cat. ab34170, Cambridge, MA), rabbit anti-collagen type IV (1:500, Abcam, Cat. ab6586, Cambridge, MA), rabbit anti-CD31 (1:350, Abcam, Cat. ab28364, Cambridge, MA), rabbit anti-elastin (1:500, Abcam, Cat. ab21610, Cambridge, MA), sheep anti-CD73 (1:350, R & D Systems, Cat. AF4488, Minneapolis, MN), mouse anti-osteocalcin (1:400, ThermoFisher Scientific, Cat. MA1–20786, Pittsburgh, PA), mouse anti-✔-SMA (1:500, Abcam, Cat. ab7817, Cambridge, MA), rabbit anti-TPPP (1:350, antibodies-online, Cat. ABIN925874, Atlanta, GA), and rat anti-substance P (1:500, Bio-RAD, Cat. 8450–0505, Farmingdale, NY) overnight at 4 °C. Sections were then washed twice in PBS for 5 min before being incubated with secondary antibody. Cy3-conjugated donkey anti-sheep IgG secondary antibody (1:500, Millipore Sigma, Cat. AP184C, Burlington, MA) was used for CD73 testing. Cy3-conjugated goat anti-mouse IgG secondary antibody (1:500, Millipore Sigma, Cat. AP124C, Burlington, MA) was used for ✔-SMA, osteocalcin, CD146, and CD105 testing. FITC-conjugated goat anti-rabbit IgG secondary antibody (1:500, ThermoFisher Scientific, Cat. F-2765, Waltham, MA) was used for CD31, elastin, and collagen I testing. Cy3-conjugated goat anti-rabbit IgG secondary antibody (1:500, Millipore Sigma, Cat. AP132C, Burlington, MA) was used for collagen IV, and TPPP testing. Cy3-conjugated goat anti-rat IgG secondary antibody (1:500, Millipore Sigma, Cat. Ap136C, Burlington, MA) was used for SP testing. All secondary antibodies were incubated for 2 hrs with the appropriate slides at room temperature. Slides were washed again, counterstained with Hoechst H33342 (Sigma, St. Louis, MO) nuclear stain, and photographed on a fluorescence microscope (Nikon eclipse, TE2000-U). Negative staining images were generated for elastin and CD73 antibodies by omitting primary antibodies, followed by incubating tissue sections with the same concentrations of secondary antibodies at the same conditions. The control images did not show any real signal, with only minor background staining (data not shown).

Cell isolation and culture

The paratenon was carefully collected from the surface, and IFM was separated from the collagen fascicles of the PAT under a microscope (Keeler, UK). Each tendon tissue structure was minced into small pieces approximately 1 mm^3, and digested in 1 ml of PBS containing 3 mg of collagenase type I and 4 mg of dispase as described previously (Zhang and Wang 2010). Following centrifugation, the cell pellets were re-suspended with Dulbecco's modified Eagle's medium (DMEM) (Invitrogen, Carlsbad, CA) supplemented with 20% fetal bovine serum (FBS) (Gibco, Grand Island, NY) and cultured in dishes or T25 flasks in 5% CO_2 at 37°C.

Cell proliferation measurement

After 14 days in culture, cells at passage 0 from the paratenon, IFM, and collagen fascicles were rinsed twice with PBS for 5 min, fixed in 4% paraformaldehyde for 15 min and then stained with methyl violet for 30 min. After rinsing twice with PBS for 5min, colonies were visualized and then counted manually. Cell proliferation assays with passage-2 cultures were analyzed for population doubling time (PDT) according to our published protocol (Zhang and Wang 2010), thus colony forming properties were evaluated by analyzing colony numbers/mg tissue. Briefly, three cell populations isolated from paratenon, IFM, and fascicles were seeded into 6-well plates with a density of 5×10^4 cells/well at passage 1. After five days in culture, the medium was removed, cells were treated with trypsin, and the cell numbers were counted by an automated cell counter (Nexcelom Bioscience, Lawrence, MA). The PDT was calculated using the equation: (T2-T1)/3.32 × (logN2 − logN1), where T1 was the culture starting time, T2 was the culture end time, N1 is the number of cells seeded, and N2 is the collected cell numbers. Each individual experiment was performed at least three times.

Cell multi-differentiation potential analysis

The multi-differentiation potentials of the cells isolated from paratenon, IFM, and collagen fascicles were examined *in vitro* to determine whether they could undergo adipogenesis, osteogenesis, and chondrogenesis. Cells at passage 2 were seeded in a 24-well plate at a density of 6×10^4 cells/well with DMEM (low glucose) consisting of 10% heat inactivated FBS, 100 U/ml penicillin, and 100 μg/ml streptomycin. After reaching confluence, the cells were cultured with three separate differentiation media for 21 days with media being changed every three days. For adipogenesis, the cells were cultured in adipogenic induction medium (Millipore, Cat. #SCR020) consisting of DMEM (low glucose) supplemented with 1 μM dexamethasone, 10 μg/ml insulin, 100 μM indomethacin, and 0.5 mM isobutylmethylxanthine (IBMX) for 21 days. Oil Red O assay (Millipore, Cat. #90358) was used to detect lipid drops contained in the differentiated adipocytes according to our published protocol (Zhang et al. 2011).

For osteogenesis, the cells were cultured with osteogenic induction medium consisting of DMEM (low glucose) with 100 nM dexamethasone, 0.2 mM ascorbic 2-phosphate, and 10 mM glycerol 2-phospahte for 21 days. The differentiated cells released calcium-rich deposits, which were stained by Alizarin Red S (Millipore, Cat. 2003999) according to our published protocol (Zhang et al. 2011).

For chondrogenesis, confluent cells were cultured in chondrogenic induction medium consisting of DMEM (low glucose) with 40 μg/ml proline, 39 ng/ml dexamethasone, 10 ng/ml transforming growth factor beta 3 (TGF-β3), 50 μg/ml ascorbic acid 2-phosphate, 100 μg/ml sodium pyruvate, and 50 mg/ml ITS premix (BD, Cat. #354350). After 21 days in culture, proteoglycans-rich matrix produced by differentiated chondrocytes was stained with Safranin O (Sigma, Cat. #HT904) according to our published protocol (Zhang et al. 2011).

Immunocytochemical analysis of cell markers

The characterizations of the cells isolated from three structural components of the tendon were further analyzed by immunocytochemistry (ICC) staining with specific cell markers. Isolated cells at passage 2 were seeded into 12-well plate at a density of 3×10^4 cells/well and cultured with DMEM medium containing 20% FBS for one week. To maintain the 'stemness' of isolated stem/progenitor cells, high concentrations of FBS-containing medium is necessary (Zhang and Wang 2010). The cells were washed for 5 min twice in PBS and fixed with 4% paraformaldehyde in PBS for 30 min at room temperature. The fixed cells were incubated separately with the following antibodies: sheep anti-CD73 (1:350, R & D Systems, Cat. AF4488, Minneapolis, MN), mouse anti-CD146 (1:500, BioRAD, Cat. MCA2141), mouse anti-CD105 (1:500, Abcam, Cat. ab69772, Cambridge, MA), mouse anti-collagen type I (1:500, Abcam, Cat. ab34170, Cambridge, MA), rabbit anti-collagen type IV (1:500, Abcam, Cat. ab6586, Cambridge, MA), rabbit anti-CD31 (1:350, Abcam, Cat. ab28364, Cambridge, MA), and rabbit anti-elastin (1:500, Abcam, Cat. ab21610, Cambridge, MA) overnight at 4 °C. The cells were then washed twice in PBS for 5 min before being incubated with secondary antibodies. Cy3-conjugated donkey anti-sheep IgG secondary antibody (1:500, Millipore Sigma, Cat. AP184C, Burlington, MA) was used for CD73 testing. Cy3-conjugated goat anti-mouse IgG secondary antibody (1:500, Millipore Sigma, Cat. AP124C, Burlington, MA) was used for CD146 and CD105 testing. Cy3-conjugated goat anti-rabbit IgG secondary antibody (1:500, Millipore Sigma, Cat. AP132C, Burlington, MA) was used for collagen IV and elastin testing. All secondary antibodies were incubated with the appropriate cells for 2 hrs at room temperature. The cells were washed again, counterstained with H33342 (Sigma, St. Louis, MO) nuclear stain, and photographed with fluorescence microscope (Nikon eclipse, TE2000-U).

Semi-quantification of positively stained tissue sections

To quantify cell marker staining *in vivo*, we used a semi-quantitative method. First, we obtained five randomly selected images from each tissue section stained for each cell marker using a fluorescence microscope (Nikon eclipse, TE2000-U). Then, positive staining in each image was identified using SPOT imaging software (Diagnostic Instruments, Inc., Sterling Heights, MI). The proportion of positive staining was calculated by dividing the total area viewed under the microscope by the positively stained area. Three sections were tested for each cell marker. The final percentage of positive staining was derived by averaging the values from all 15 images.

Semi-quantification of positively stained cells

To quantify cell marker staining *in vitro*, we used the similar semi-quantitative method as described above for tissue section staining. Three random images were taken from each well using the same equipment and software as described above. The percentage of positive staining in each image was estimated by dividing the number of positively stained cells by the total number of cells counterstained with H33342 (1 μg/ml; Sigma, St. Louis, MO) in the microscopic field, and multiplying by 100. Three wells were used for each marker staining. The final percentage of positive staining was derived by averaging the values from all 9 images.

Statistical analysis

Data are expressed as means ± standard deviations (SD). For statistical analysis, one-way ANOVA were performed followed by Fisher's least significant difference (LSD) test. Statistical significance was defined by the value of $p < 0.05$.

Results

Dissection and gross anatomy of PAT displays three distinct components

A gross examination of young juvenile 6-month old porcine Achilles tendon indicated that the tendon is a few millimeters thick, consisting of a pearly white, glistening layer of fiber bundles, connecting the calcaneus with the leg muscle tissue (Fig. 1a). The tendon displayed the typical structural features of human Achilles tendon. The surface of the Achilles tendon was covered with paratenon (red arrows in Fig. 1a, b, d), the core part under the paratenon was formed by collagen fascicles (blue arrows in Fig. 1b, c), with the IFM comprised of membrane-like structures between the fascicles (yellow arrows in Fig. 1b, c). When the paratenon and IFM were removed, the white collagen fibers remained (pink arrow in Fig. 1e). Further characterization of Achilles tendon was performed using histochemical staining and immunostaining.

Histological staining and structural assessment of tendon tissue sections

Staining of cross and longitudinal sections showed that PAT consists of at least three distinct components (Fig. 2). The outside tendon is surrounded by a loose sheath representing the paratenon (black arrows in Fig. 2a, d), with some blood vessel-like tissues extended from the paratenon (green arrows in Fig 2a, d) to the IFM (green arrows in Fig. 2b, e). The core tissues are formed by high density collagen fiber bundles, *i.e.* forming collagen fascicles (blue arrows in Fig. 2a–f), with the loose net-like structure of the IFM forming between tendon fascicles (red arrows in Fig. 2a–f). Finally, the morphology of cells within collagen fibers are elongated in shape (yellow arrows in Fig. 2f), while cells within the IFM are round shape (white arrows in Fig. 2f).

These findings were further confirmed by Safranin O and Fast Green staining showing three separate components. Similar to the H&E staining results, the tendon surface was covered by the loose sheath of the paratenon (yellow arrows in Fig. 3a), and some blood vessel-like tissues also extended from the paratenon to the IFM (black arrows in Fig. 3a–d, g–h). The core component of the tendon was formed by high density collagen fiber bundles shown by staining with Fast Green (Fig. 3). In contrast to these closely packed fiber bundles, the IFM again showed a loose net-like mesh structure between the collagen fiber bundles as evidenced by Safranin O staining (red arrows in Fig. 3).

Similar results were obtained by using a scanning electron microscope (SEM) to obtain clear and highly detailed images of cross and longitudinal sections of PAT. The loose net-like mesh of the IFM (red arrows in Fig. 4a, c, d, f) was found between the collagen fiber bundles, with some blood vessel-like structures within the IFM (yellow arrows in Fig. 4a, d, f). Many high-density collagen fiber bundles were found in core tendon tissues (white arrows in Fig. 4a, d), and were well organized into collagen fascicles (green arrows in Fig.

4b, e). Overall, the structures of the collagen fascicles (green arrow in Fig. 4b) and IFM (red arrow in Fig. 4c) are different.

Next, cross tissue sections of each component were analyzed for collagen I (green fluorescence) and collagen IV content (red fluorescence), with results showing a clear separation between the paratenon, IFM, and fascicle components (Fig. 5a–c). Paratenon tissues stained for collagen IV (Fig. 5d, f) and collagen I (Fig. 5e, f). The net-like IFM tissues were also positively stained for collagen type IV (Fig. 5g, i), but relatively lower level for collagen type I (white arrows in Fig. 5h, i). Finally, fascicle tissues showed high level of positive staining for collagen type I (Fig. 5h, i), but none for collagen IV (blue arrows in Fig. 5g, i). Overall, the merged image (Fig. 5i) combined with semi-quantification (Fig. 5j) shows a clear net-like IFM (white arrows) staining with high levels of collagen IV and low levels of collagen I thus producing an overall orange color, with this IFM resting between fascicles (blue arrows), and fascicles staining with high levels of collagen I only.

Immunostaining of tendon components for the presence of vascular markers, blood vessel-like structures, and structure-specific stem cells

Each component within PAT was assessed for the presence of stem cells and blood vessel-like structures in cross and longitudinal tissue sections. Initial experiments focused on analyzing sections for the presence of elastin (green fluorescence) and $CD73^+$ surface marker for mesenchymal stem cells (MSCs; red fluorescence). Paratenon and net-like IFM tissue stained positively for both elastin and CD73 (Fig. 6a–d). Fascicles were negatively stained with CD73 (white arrows indicating black/unstained regions in Fig. 6b, c, f, g), with only a few fascicles stained positively for elastin. Some blood vessel-like tissues were found in IFM, with the interior surfaces of these structures positively stained with elastin and the exterior positively stained with CD73 (yellow arrows in Fig. 6e–h). Some large areas were positively stained with CD73 due to a high density of $CD73^+$ cells. Similar results can be found elsewhere (Monteiro et al. 2018; Tan et al. 2019). Semi-quantification supports these results, showing elevated levels of elastin and CD73 within both the paratenon and IFM tissues in comparison to minimal levels within fascicles (Fig. 6i).

Cross-sectional tissue sections (Fig. 7) showed evidence of pericytes (CD105, red fluorescence) and blood vessels (CD31, green fluorescence) within specific components. Phase contrast imaging (Fig. 7a, f) and H33342 staining (blue in Fig. 7b, g) shows a clear separation of the paratenon, IFM, blood vessels, and fascicles. Paratenon tissues were stained positively for both CD105 and CD31 (Fig. 7h–j). Overall net-like IFM tissues contained both pericytes and blood vessels, as evidenced by CD105 and CD31 markers (Fig. 7c–e, h–j) concentrated on the interior of these blood vessel tissues (white arrows in Fig. 7c–e). However, fascicle tissues did not show staining for either CD105 or CD31, suggesting that they may not contain pericytes or vessels (empty areas in Fig. 7c–e, h–j). Semi-quantification of these results supports our immunostaining findings, showing elevated CD31 and CD105 within both the paratenon and IFM, and low levels within fascicles (Fig. 7k).

Cross section staining results were analyzed for the presence of CD146 endothelial marker (red fluorescence) and collagen type I (green fluorescence), again showing a clear separation

of the paratenon, IFM, and fascicle structures (labeled with arrows in Fig. 8a). The paratenon and IFM were stained positively for both CD146 and collagen type I markers (Fig. 8b–e), and fascicles were stained with collagen I only (yellow arrows and white outlined structures Fig. 8b–e). Semi-quantification was performed on images **a-d**, showing that IFM is enriched for CD146 in contrast to fascicles which were enriched for collagen I (Fig. 8f). Longitudinal sections further confirmed our CD146 staining results. IFM structures displayed a higher level of staining for endothelial cell marker CD146 (white outlined structure in Fig. 8g–i) but a few fascicle cells were also positively stained with CD146 (white arrows in Fig. 8g–i).

Osteocalcin, α-SMA, and TPPP expression in PAT

We assessed cross and longitudinal sections of each component for the presence of osteocalcin (Wang et al. 2017), tubulin polymerization promoting protein (TPPP) (Harvey et al. 2019; Staverosky et al. 2009), and α-SMA (Bi et al. 2007; Dyment et al. 2014; Geevarghese and Herman 2014; Grcevic et al. 2012) (red fluorescence in Fig. 9), all previously described markers that are present within TSCs. Osteocalcin was found within the paratenon (white double-headed arrow in Fig. 9a) and IFM tissues (Fig. 9b–e), and negatively stained in fascicles (green arrows in Fig. 9a–e). Smooth muscle actin (α-SMA) was only positively stained in surrounding blood vessel-like tissues within the paratenon (Fig. 9f) and IFM (Fig. 9g–j), while overall IFM and fascicles (green arrows) were negatively stained with α-SMA (Fig. 9f–j). Additional staining was carried out for tubulin polymerization promoting protein (TPPP) staining. Our results show that paratenon tissues (Fig. 9k) were highly stained for TPPP, with a low level of staining within some IFM tissues (Fig. 9l–o). However, fascicles were not positively stained with TPPP (green arrows in Fig. 9k–o). Semi-quantification of this data shows the paratenon and IFM to be predominant components that express each of these markers (Fig. 9p). This is in contrast to fascicles, which exhibited only minimal levels of each.

Localization of Substance P within tendon components

Our results show that substance P (SP) was localized specifically surrounding blood vessel-like structures (red fluorescence) within the paratenon (Fig. 10a, e) and IFM (Fig. 10b–d, f–h), but the fascicles (white arrows) and overall IFM tissues (yellow arrows) were negatively stained (Fig. 10 b–d, f–h). Again, semi-quantification supports our results, showing that SP is highly expressed within the paratenon and IFM tissues compared to fascicles (Fig. 10i). With our combined immunostaining results, our data suggests that paratenon, IFM, and fascicles perform different yet complementary functions. Table 1 summarizes the data from Figs. 1–10 of the analysis of tissue sections.

Immunostaining of *in vitro* cell populations from paratenon, IFM, and fascicles

Cells were isolated from each specific component, cultured, and analyzed for differences in morphology and population doubling time (PDT). In general, individual stem/progenitor cells give rise to colonies, however mature or fully differentiated cells do not. Primary cultures showed that cells isolated from paratenon were endothelial-like cells (Fig. 11a), and cells isolated from the IFM exhibited cobblestone-like morphology and formed colonies

with the typical features of stem cells (Fig. 11b). Fascicle cells were elongated in shape without forming colonies (Fig. 11c), and exhibited characteristics of fibroblast-like cells as suggested by their morphology, multi-differentiation potential, and population doubling time (PDT). After 21 days in three differentiation media, both paratenon cells and IFM cells expressed lipid droplets (Fig. 11d, e), calcium-rich deposits (Fig. 11g, h), and proteoglycans (Fig. 11j, k). However, only a few fascicle cells were positively stained for lipid droplets (Fig. 11f), calcium-rich deposits (Fig. 11i), and proteoglycans (Fig. 11l).

With additional culturing, passage 2 cells were utilized for PDT analysis, with results showing paratenon cells produced the shortest PDT of the three populations. Thus, paratenon cells grew faster than the other two cell populations as indicated by PDT values of the three populations of cells (Fig. 11m). Thus, each tendon component displayed a unique property in terms of cell morphology and PDT.

Additional staining was performed on isolated cells from each component for specific stem cell and vascular markers. Our results showed that although all three cell populations expressed elastin, elevated levels can be seen in the paratenon and IFM cells in comparison to lower levels within fascicle cells (Fig. 12a–c). The paratenon and IFM cells expressed high levels of collagen IV (Fig. 12d, e), with only a few fascicle cells expressing collagen IV (Fig. 12f). The paratenon also expressed collagen type I (Fig. 12g), however the relative level of expression was lower, compared to fascicle cells that expressed high levels of collagen type I (Fig. 12i). IFM cells, on the other hand, did not have any collagen type I staining (Fig. 12h). Our data is supported by semi-quantification of these slides, showing elevated elastin and collagen IV within the paratenon and IFM tissues, and elevated levels of collagen I within fascicles (Fig. 12j).

Finally, isolated cells were assessed for the expression of specific stem cell and vascular markers. Both paratenon and IFM cells expressed CD73 (Fig. 13a, e) and CD146 (Fig. 13b, f) to similar levels, however only a few fascicle cells were positively stained for both markers (Fig. 13i, j). Furthermore, both paratenon and IFM cells expressed vascular cell markers CD105 (Fig. 13c, g) and CD31 (Fig. 13d, h) to similar levels, with fascicle cells expressing CD31 at much lower levels (Fig. 13l) without any expression of CD105 (Fig. 13k). Overall, both the paratenon and IFM isolated cell cultures contained vascular stem/progenitor cell populations, in direct contrast with isolated fascicle cells, and is supported by our semi-quantification of this data (Fig. 13m). These results are in agreement with immunohistochemical results of the porcine Achilles tendon in Table 1. *In vitro* results from Figs. 11–13 are summarized in Table 2.

Discussion

Considering the lack of sufficient understanding of the tendon substructure, we characterized juvenile porcine midportion Achilles tendons in terms of their detailed structure, vascularity, and presence of specific vascular stem cells. Specifically, structural analysis of the paratenon and IFM showed a loose membrane-like tissue interconnected with blood vessels extending from the paratenon into the net-like IFM, in contrast to well-organized collagen fascicles that lacked vascularity. In addition to the similarity in overall structure and vascularity,

paratenon and IFM harbor similar stem/progenitor cell populations, specific collagen IV content, and localization of SP within blood vessel structures. In contrast, fascicles with high collagen I lack the above characteristics. The cells isolated from each structure component also displayed differential properties in terms of their morphology, multi-differentiation potential, stem cell marker expression, and proliferation.

Tendon is generally described as a hypovascular structure, however specific substructures of tendon does contain evidence of vascularity (Ahmed et al. 1998; Doral et al. 2010; Fenwick et al. 2002). Our findings on the structural analyses of PAT show the presence of blood vessel-like structures extending from the paratenon into the IFM. This is in agreement with similar structural studies, including human Achilles tendon, detailing a highly vascularized paratenon, with blood vessels running from the outer layers into the endotenon (IFM), surrounding avascular collagen fiber bundles or fascicles, as discussed in great detail elsewhere (Ahmed et al. 1998; Dederer and Tennant 2019; Doral et al. 2010; Fenwick et al. 2002). Our results are consistent with previous findings supporting tendon vascularization (Benjamin et al. 2008; Fenwick et al. 2002; Tempfer and Traweger 2015) as well as a recent study showing vascularization of the IFM within the equine superficial digital flexor tendon and common digital extensor tendons (Godinho et al. 2017). The study of tendon vascularity has been used to make conclusions about tendon repair, with research suggesting that the level of vascularity is linked to the level or quality of tendon healing and repair at the site of injury. Cells isolated from the peritenon (the combined structure of the paratenon and epitenon) or perivascular structures have been shown to express cell markers related to both mature tendon tissue and mesenchymal stem cells (Tempfer et al. 2009), as well as exhibiting clonogenicity and multipotency (Zhang et al. 2019). While it is understood that the paratenon in young adult human tendon is highly vascularized, vascularity decreases with age leading to poorly vascularized tendon (Fenwick et al. 2002). Tendon vascularity, such as in Achilles tendon, is not uniform throughout the entirety of the tendon, which is considered to be a reason why human midportion tendon region, weakened by tendinopathic lesions, is highly susceptible to rupture (Dederer and Tennant 2019; Doral et al. 2010). Our results showed that vascularity is present in midportion PAT, but this vascularity is not uniform between all three substructures; the paratenon and IFM are vascular as shown through structural studies and the presence of vascular cells within them, while the tendon core region, *i.e.* the fascicles, is largely avascular.

Our data also shows that paratenon and IFM contain high levels of collagen IV, in contrast to core fascicle tissues with no collagen IV, but high levels of collagen I. Since collagen IV is an integral component of vascular basement membrane (Boudko et al. 2018), our observation further substantiates that paratenon and IFM indeed harbor vessels. The paratenon and IFM had relatively lower level of collagen I compared to that in fascicles. The main components of paratenon are known to be collagen I and III (Kannus 2000; Williams 1986), and IFM also contains small amounts of a variety of collagens including collagen I and III (Sodersten et al. 2013; Thorpe et al. 2016a). However, collagen III can also be found in low amounts within fascicles (Thorpe et al. 2016a), making it an imperfect marker for this immunostaining research when attempting to characterize unique or separate markers for each component. We also found higher levels of elastin in paratenon and IFM compared to low levels in fascicles. Elastin is sparsely distributed in fascicles (Kannus 2000), but it is

concentrated within the IFM in equine models, and contributes to the overall elasticity within this structure by facilitating sliding and recoiling between fascicles (Godinho et al. 2017; Thorpe et al. 2016b). Thus, our data clearly show that the IFM contains high levels of elastin.

Substance P (SP) is a mechanoresponsive neuropeptide known to be found in the area of nerve fascicles and fibers surrounding blood vessels, and is known to be involved in tendon pain (Andersson et al. 2007; Andersson et al. 2008). SP plays a role in pain transmission, cell growth and angiogenesis (Fan et al. 1993), vasodilation and increased vascular permeability (Lam and Yip 2000), as well as a role in improved healing in rat Achilles tendon (Burssens et al. 2005; Steyaert et al. 2006). SP has also been shown to be present in the region surrounding blood vessels in the paratenon and epitenon of human healthy and tendinopathic mid-portion Achilles tendon tissues (Ackermann et al. 2003; Ackermann 2016; Bjur et al. 2005), and may play a role in fibrotic tendon healing and pain (Barbe et al. 2019). Our results support this localization of SP, showing expression in and around blood vessels within the paratenon and IFM but lacking in fascicles, suggesting a role for SP in pain transmission through blood vessels in the event of tendon injury. More research is needed in order to understand how SP and tendon vascularity impact tendon damage, healing, and repair.

With regard to the cell population in the three components, our results show the presence of specific stem cell populations, including MSC markers CD73, CD105, and CD146 (Dominici et al. 2006; Lv et al. 2014; Maleki et al. 2014; Monteiro et al. 2018; Tan et al. 2019). Both paratenon and IFM display CD73 surface marker for MSCs, while fascicles lacked the expression. Similar results were seen with vascular endothelial markers CD105 and CD31, with elevated levels of expression in the paratenon and IFM, but only minimal levels within fascicles. These results further support the presence of vascularity in paratenon and IFM, but not in fascicles. Additionally, CD146 is one of the markers that identifies TSCs (Bi et al. 2007; Rui et al. 2010; Zhang and Wang 2010). Our results show that it is highly expressed in paratenon and IFM (Fig. 8f), and at minimal levels in fascicles. Previous studies have identified distinct populations of TSCs either from the paratenon or tendon proper suggesting that different progenitor populations exist within distinct niches at the tendon proper and paratenon (Cadby et al. 2014; Mienaltowski et al. 2013; Tan et al. 2013; Walia and Huang 2019; Zhang et al. 2019).

Osteocalcin, α-SMA, and TPPP are markers that have been presented in the literature as specific markers of progenitor cell populations within tendon (Dyment et al. 2014; Geevarghese and Herman 2014; Grcevic et al. 2012; Harvey et al. 2019; Staverosky et al. 2009; Wang et al. 2017). Our results show the presence of all three markers with variability between each in localization and expression level within PAT. Osteocalcin is present within the paratenon and IFM, previously described as a specific marker for tendon sheath specific stem progenitor cells in mice involved in facilitating tendon healing and repair by activating hedgehog signaling (Wang et al. 2017). Osteocalcin is strongly stained near blood vessels, suggesting that cells expressing osteocalcin may circulate throughout the tendon or elsewhere. Our results with TPPP staining, in regards to their role in tendon sheath embryonic development and as a marker for paratenon sheath tendon stem cells that

facilitate healing and repair (Harvey et al. 2019; Staverosky et al. 2009), indicate that $TPPP^+$ cells are present in both the paratenon and IFM tissues, but absent in fascicles. Our results also show localization of α-SMA surrounding blood vessels within the paratenon and IFM. Alpha-SMA is known to be highly expressed within smooth muscle cells in blood vessels, and act as a marker for tendon progenitor cells, MSCs, and perivascular cells (Bi et al. 2007; Dyment et al. 2014; Geevarghese and Herman 2014; Grcevic et al. 2012). It remains to be seen how these markers respond to tendon injury and trauma, and how these cells may migrate within the connected paratenon-IFM structure. The role of these specific cellular populations and the level of coordination that may occur between these populations in regard to responding to early or late stage tendon injuries, requires more research.

This study has certain limitations. While porcine tendon provides a clear evaluation of specific components not known to exist within rats or mice, pigs are quadruped animals, and thus a direct translation of our results to humans must be further explored through a careful comparison to human specimens. However, the ability to obtain fresh human tendon in large quantities sufficient to obtain consistent results is limited. Secondly, while we have characterized collagen fascicles in terms of collagen content and cell types, fascicles are composed of many small components, such as decorin and aggrecan. Additionally, more sensitive methods like fluorescence activated cell sorting (FACS) analysis are needed to identify and create a pool of each of these sub-populations of stem cells specific to each component. Such sophisticated analysis will overcome the limitation of this study that used only immunocytochemical analysis from cultures that may have been impure.

In conclusion, our results have shown that the vascularity of PAT substructures are not uniform throughout the tissue. While paratenon and IFM are highly vascular, these structures extend into the tendon surrounding the tendon core fascicles which are avascular. The paratenon and IFM are structurally and cellularly different from fascicles. However, it is possible that the paratenon and IFM may harbor similar but also separate sub-populations of stromal cells and tendon/stem progenitor cells that may have differential functions in tendon healing and repair. Further studies are warranted to assess how specific cell populations within each component contribute to healing and repair of tendon following injury.

Acknowledgments

Funding

The funding source for this study was in part from the National Institutes of Health under award numbers AR061395, AR065949, and AR070340 (JHW).

References

Ackermann PW, Li J, Lundeberg T, Kreicbergs A (2003) Neuronal plasticity in relation to nociception and healing of rat achilles tendon. J Orthop Res 21:432–441 [PubMed: 12706015]

Ackermann PW, Salo P, Hart DA (2016) Tendon innervation. In: Ackermann PW, Hart DA (ed) Metabolic influences on risk for tendon disorders, vol 920. Springer, pp 35–52

Ahmed IM, Lagopoulos M, McConnell P, Soames RW, Sefton GK (1998) Blood supply of the achilles tendon. Journal of Orthopaedic Research 16:591–596 [PubMed: 9820283]

Andersson G, Danielson P, Alfredson H, Forsgren S (2007) Nerve-related characteristics of ventral paratendinous tissue in chronic Achilles tendinosis. Knee Surgery, Sports Traumatology, Arthroscopy 15:1272–1279

Andersson G, Danielson P, Alfredson H, Forsgren S (2008) Presence of substance P and the neurokinin-1 receptor in tenocytes of the human Achilles tendon. Regulatory peptides 150:81–87 [PubMed: 18394729]

Barbe MF, Hilliard BA, Fisher PW, White AR, Delany SP, Iannarone VJ, Harris MY, Amin M, Cruz GE, Popoff SN (2019) Blocking substance P signaling reduces musculotendinous and dermal fibrosis and sensorimotor declines in a rat model of overuse injury. Connect Tissue Res 1–16

Benjamin M, Kaiser E, Milz S (2008) Structure-function relationships in tendons: a review. Journal of anatomy 212:211–228 [PubMed: 18304204]

Bi Y, Ehirchiou D, Kilts TM, Inkson CA, Embree MC, Sonoyama W, Li L, Leet AI, Seo BM, Zhang L, Shi S, Young MF (2007) Identification of tendon stem/progenitor cells and the role of the extracellular matrix in their niche. Nat Med 13:1219–1227 [PubMed: 17828274]

Bjur D, Alfredson H, Forsgren S (2005) The innervation pattern of the human Achilles tendon: studies of the normal and tendinosis tendon with markers for general and sensory innervation. Cell and Tissue Research 320:201–206 [PubMed: 15702331]

Boudko SP, Danylevych N, Hudson BG, Pedchenko VK (2018) Basement membrane collagen IV: Isolation of functional domains. Methods Cell Biol 143:171–185 [PubMed: 29310777]

Burssens P, Steyaert A, Forsyth R, van Ovost EJ, Depaepe Y, Verdonk R (2005) Exogenously administered substance P and neutral endopeptidase inhibitors stimulate fibroblast proliferation, angiogenesis and collagen organization during Achilles tendon healing. Foot Ankle Int 26:832–839 [PubMed: 16221456]

Cadby JA, Buehler E, Godbout C, van Weeren PR, Snedeker JG (2014) Differences between the cell populations from the peritenon and the tendon core with regard to their potential implication in tendon repair. PLoS One 9:e92474 [PubMed: 24651449]

Dederer KM, Tennant JN (2019) Anatomical and Functional Considerations in Achilles Tendon Lesions. Foot Ankle Clin 24:371–385 [PubMed: 31370991]

Dominici M, Le Blanc K, Mueller I, Slaper-Cortenbach I, Marini F, Krause D, Deans R, Keating A, Prockop D, Horwitz E (2006) Minimal criteria for defining multipotent mesenchymal stromal cells. The International Society for Cellular Therapy position statement. Cytotherapy 8:315–317 [PubMed: 16923606]

Doral MN, Alam M, Bozkurt M, Turhan E, Atay OA, Dönmez G, Maffulli N (2010) Functional anatomy of the Achilles tendon. Knee Surgery, Sports Traumatology, Arthroscopy 18:638–643

Dyment NA, Hagiwara Y, Matthews BG, Li Y, Kalajzic I, Rowe DW (2014) Lineage tracing of resident tendon progenitor cells during growth and natural healing. PLoS One 9:e96113 [PubMed: 24759953]

Fan TPD, Hu DE, Guard S, Gresham GA, Watling KJ (1993) Stimulation of angiogenesis by substance P and interleukin-1 in the rat and its inhibition by NK1 or interleukin-1 receptor antagonists. British journal of pharmacology 110:43–49 [PubMed: 7693287]

Fenwick SA, Hazleman BL, Riley GP (2002) The vasculature and its role in the damaged and healing tendon. Arthritis research 4:252–260 [PubMed: 12106496]

Geevarghese A, Herman IM (2014) Pericyte-endothelial crosstalk: implications and opportunities for advanced cellular therapies. Translational research : the journal of laboratory and clinical medicine 163:296–306 [PubMed: 24530608]

Godinho MSC, Thorpe CT, Greenwald SE, Screen HRC (2017) Elastin is Localised to the Interfascicular Matrix of Energy Storing Tendons and Becomes Increasingly Disorganised With Ageing. Scientific reports 7:9713–9713 [PubMed: 28855560]

Grcevic D, Pejda S, Matthews BG, Repic D, Wang L, Li H, Kronenberg MS, Jiang X, Maye P, Adams DJ, Rowe DW, Aguila HL, Kalajzic I (2012) In vivo fate mapping identifies mesenchymal progenitor cells. Stem Cells 30:187–196 [PubMed: 22083974]

Harvey T, Flamenco S, Fan C-M (2019) A Tppp3+Pdgfra+ tendon stem cell population contributes to regeneration and reveals a shared role for PDGF signalling in regeneration and fibrosis. Nature Cell Biology 21:1490–1503 [PubMed: 31768046]

Kannus P (2000) Structure of the tendon connective tissue. Scandinavian Journal of Medicine & Science in Sports 10:312–320 [PubMed: 11085557]

Kapetanakis S, Gkasdaris G, Daneva E, Givissis P, Papathanasiou J, Xanthos T (2017) Mechanoreceptors of the Achilles tendon: a histomorphological study in pigs with clinical significance for humans. Muscles Ligaments Tendons J 7:558–563 [PubMed: 29721457]

Lam FF, Yip AL (2000) Unique gradual and sustained vasodilator response to substance P in the rabbit knee joint. European journal of pharmacology 400:327–335 [PubMed: 10988351]

Lv FJ, Tuan RS, Cheung KM, Leung VY (2014) Concise review: the surface markers and identity of human mesenchymal stem cells. Stem Cells 32:1408–1419 [PubMed: 24578244]

Maffulli N, Sharma P, Luscombe KL (2004) Achilles tendinopathy: aetiology and management. J R Soc Med 97:472–476 [PubMed: 15459257]

Maleki M, Ghanbarvand F, Reza Behvarz M, Ejtemaei M, Ghadirkhomi E (2014) Comparison of mesenchymal stem cell markers in multiple human adult stem cells. Int J Stem Cells 7:118–126 [PubMed: 25473449]

Mienaltowski MJ, Adams SM, Birk DE (2013) Regional differences in stem cell/progenitor cell populations from the mouse achilles tendon. Tissue engineering Part A 19:199–210 [PubMed: 22871316]

Monteiro I, Vigano S, Faouzi M, Treilleux I, Michielin O, Ménétrier-Caux C, Caux C, Romero P, de Leval L (2018) CD73 expression and clinical significance in human metastatic melanoma. Oncotarget 9:

Nichols AEC, Best KT, Loiselle AE (2019) The cellular basis of fibrotic tendon healing: challenges and opportunities. Translational Research 209:156–168 [PubMed: 30776336]

Rui YF, Lui PP, Li G, Fu SC, Lee YW, Chan KM (2010) Isolation and characterization of multipotent rat tendon-derived stem cells. Tissue Eng Part A 16:1549–1558 [PubMed: 20001227]

Snedeker JG, Foolen J (2017) Tendon injury and repair – A perspective on the basic mechanisms of tendon disease and future clinical therapy. Acta Biomaterialia 63:18–36 [PubMed: 28867648]

Sodersten F, Hultenby K, Heinegard D, Johnston C, Ekman S (2013) Immunolocalization of collagens (I and III) and cartilage oligomeric matrix protein in the normal and injured equine superficial digital flexor tendon. Connect Tissue Res 54:62–69 [PubMed: 23020676]

Staverosky JA, Pryce BA, Watson SS, Schweitzer R (2009) Tubulin polymerization-promoting protein family member 3, Tppp3, is a specific marker of the differentiating tendon sheath and synovial joints. Developmental Dynamics 238:685–692 [PubMed: 19235716]

Steyaert AE, Burssens PJ, Vercruysse CW, Vanderstraeten GG, Verbeeck RM (2006) The Effects of Substance P on the Biomechanic Properties of Ruptured Rat Achilles' Tendon. Archives of Physical Medicine and Rehabilitation 87:254–258 [PubMed: 16442981]

Tan K, Zhu H, Zhang J, Ouyang W, Tang J, Zhang Y, Qiu L, Liu X, Ding Z, Deng X (2019) CD73 Expression on Mesenchymal Stem Cells Dictates the Reparative Properties via Its Anti-Inflammatory Activity. Stem Cells International 2019:8717694 [PubMed: 31249602]

Tan Q, Lui PPY, Lee YW (2013) In vivo identity of tendon stem cells and the roles of stem cells in tendon healing. Stem cells and development 22:3128–3140 [PubMed: 23815595]

Tempfer H, Traweger A (2015) Tendon Vasculature in Health and Disease. Front Physiol 6:330 [PubMed: 26635616]

Tempfer H, Wagner A, Gehwolf R, Lehner C, Tauber M, Resch H, Bauer HC (2009) Perivascular cells of the supraspinatus tendon express both tendon- and stem cell-related markers. Histochemistry and Cell Biology 131:733–741 [PubMed: 19280209]

Theobald P, Benjamin M, Nokes L, Pugh N (2005) Review of the vascularisation of the human Achilles tendon. Injury 36:1267–1272 [PubMed: 16214470]

Thorpe CT, Peffers MJ, Simpson D, Halliwell E, Screen HR, Clegg PD (2016a) Anatomical heterogeneity of tendon: Fascicular and interfascicular tendon compartments have distinct proteomic composition. Sci Rep 6:20455 [PubMed: 26842662]

Thorpe CT, Riley GP, Birch HL, Clegg PD, Screen HRC (2016b) Fascicles and the interfascicular matrix show adaptation for fatigue resistance in energy storing tendons. Acta Biomater 42:308–315 [PubMed: 27286677]

Walia B, Huang AH (2019) Tendon stem progenitor cells: Understanding the biology to inform therapeutic strategies for tendon repair. J Orthop Res 37:1270–1280 [PubMed: 30270569]

Wang Y, Zhang X, Huang H, Xia Y, Yao Y, Mak AF, Yung PS, Chan KM, Wang L, Zhang C, Huang Y, Mak KK (2017) Osteocalcin expressing cells from tendon sheaths in mice contribute to tendon repair by activating Hedgehog signaling. Elife 6:

Williams JG (1986) Achilles tendon lesions in sport. Sports Med 3:114–135 [PubMed: 3515485]

Yin Z, Hu JJ, Yang L, Zheng ZF, An CR, Wu BB, Zhang C, Shen WL, Liu HH, Chen JL, Heng BC, Guo GJ, Chen X, Ouyang HW (2016) Single-cell analysis reveals a nestin(+) tendon stem/progenitor cell population with strong tenogenic potentiality. Sci Adv 2:e1600874 [PubMed: 28138519]

Zhang C, Zhu J, Zhou Y, Thampatty BP, Wang JHC (2019) Tendon Stem/Progenitor Cells and Their Interactions with Extracellular Matrix and Mechanical Loading. Stem cells international 2019:3674647–3674647 [PubMed: 31737075]

Zhang J, Pan T, Im H-J, Fu FH, Wang JHC (2011) Differential properties of human ACL and MCL stem cells may be responsible for their differential healing capacity. BMC Medicine 9:68 [PubMed: 21635735]

Zhang J, Wang JH (2010) Characterization of differential properties of rabbit tendon stem cells and tenocytes. BMC Musculoskelet Disord 11:10 [PubMed: 20082706]

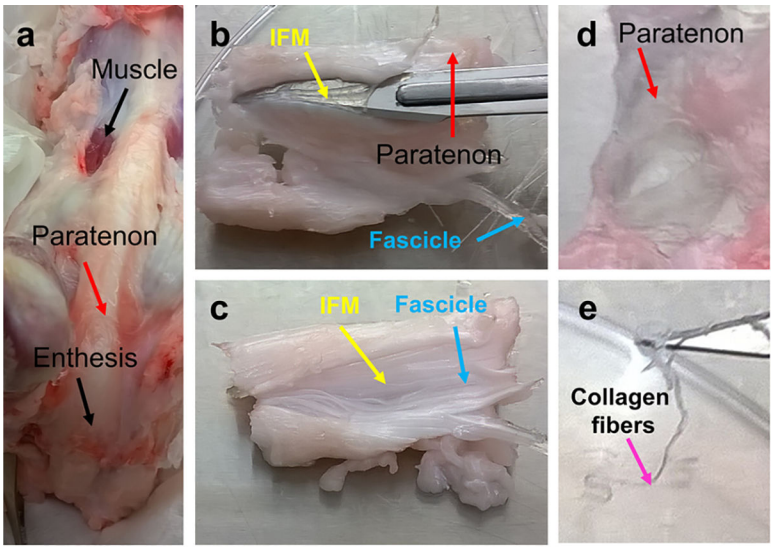

Fig. 1. Gross examination of PAT.

Gross examination shows typical structural features of the Achilles tendon with three distinct compartments (**a**). The surface of the PAT is covered with paratenon (red arrows in **a, b, d**), the core part under the paratenon is formed by collagen fascicles (blue arrows in **b, c**), and the IFM with membrane-like structures are found between the fascicles (yellow arrows in **b, c**). When paratenon and IFM are removed, the white collagen fibers are left (pink arrow in **e**).

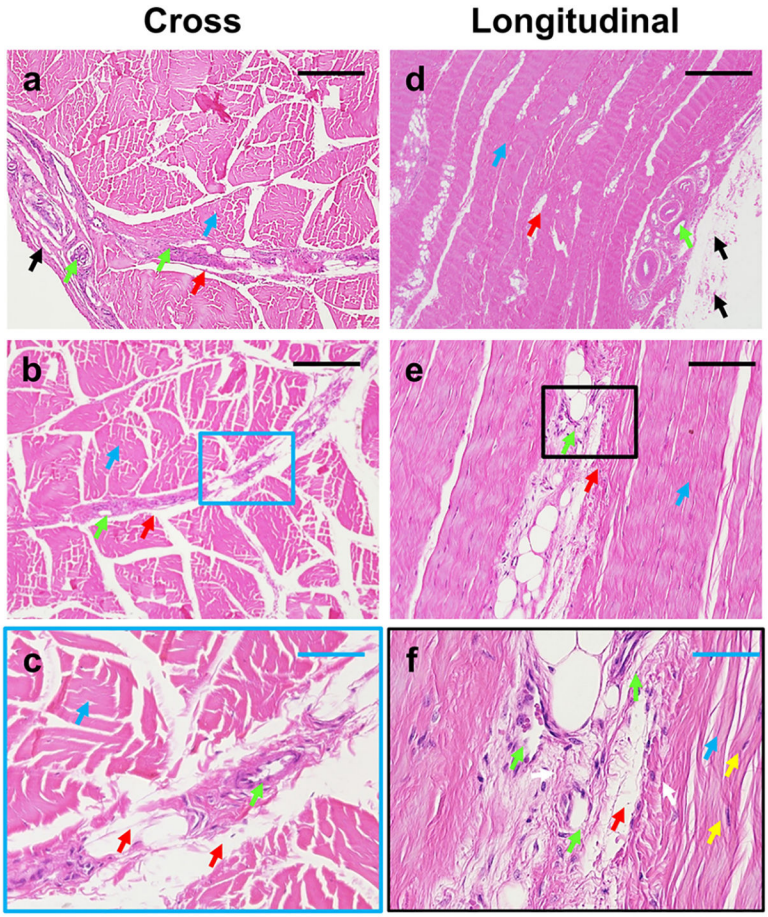

Fig. 2. Histological analysis of PAT by H&E staining of cross and longitudinal tissue sections.

The results show that the PAT at least has three different components: paratenon, IFM, and fascicles. The tendon surface is covered by the paratenon (black arrows in **a, d**), with the loose net-mesh of the IFM between the collagen fiber bundles (red arrows in **a-f**). The core tendon structure is formed by high-density collagen fiber bundles (blue arrows in **a-f**). Some blood vessel-like tissues extend from the paratenon (green arrows in **a, d**) to the IFM (green arrows in **b, c**). The cells in the collagen fibers are elongated in shape (yellow arrows in **f**), however, the cells in IFM exhibit a round shape (white arrows in **f**). Images **a**, **b**, **d**, and **e** represent separate tissue sections. Image **c** is the enlarged image of **b**, with a correlating blue box. Image **f** is the enlarged image of the black box in image **e**. Black bars: 200 μm; Blue bars: 50 μm.

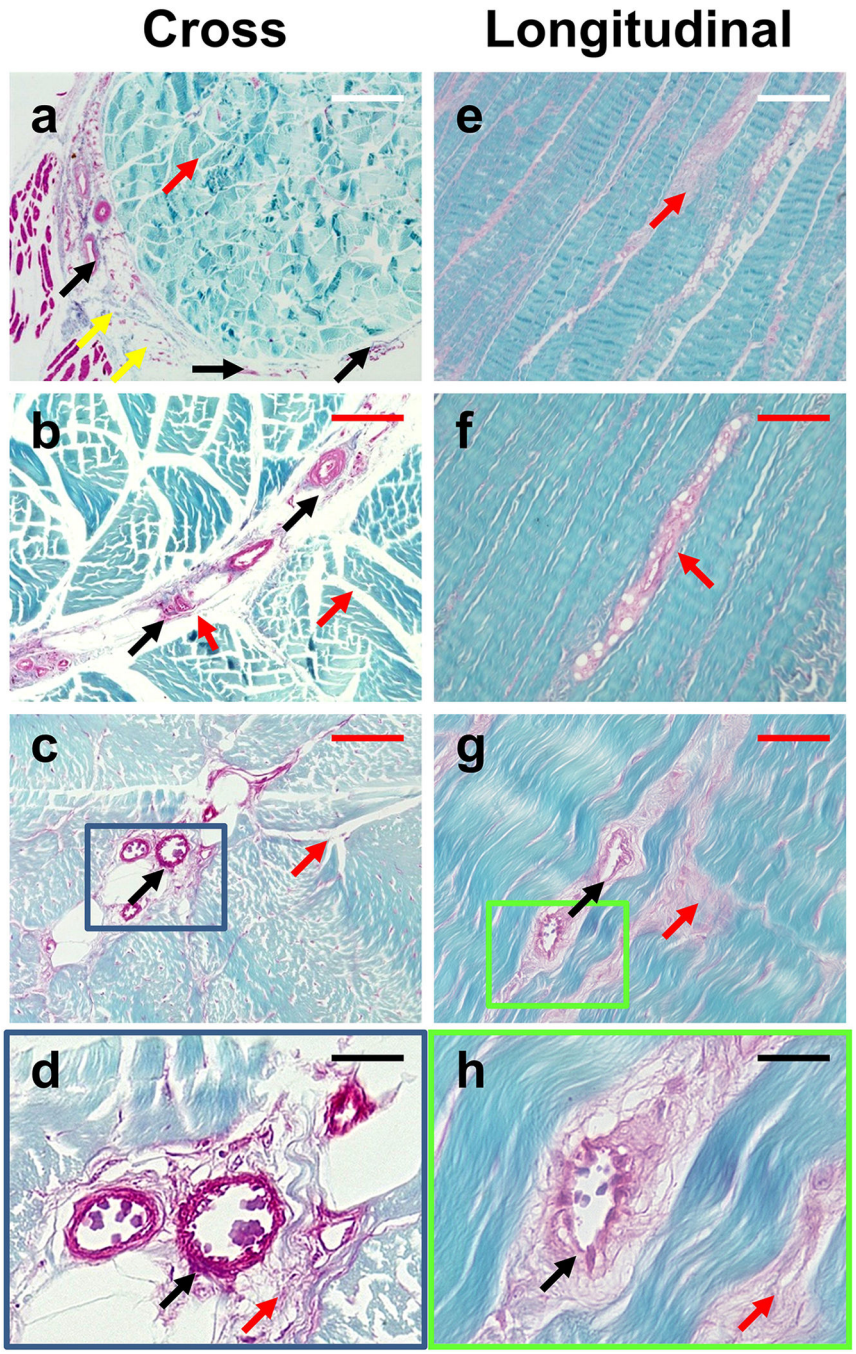

Fig. 3. Histological analysis of PAT by Safranin O & Fast Green staining of cross and longitudinal tissue sections.

Results show that the PAT at least has three different components, with the tendon surface covered by paratenon (yellow arrows in **a**), and a loose net-mesh of the IFM between the collagen fiber bundles (red arrows), and a core component formed by high-density collagen fiber bundles stained with fast green. Some blood vessel-like tissues are extended from paratenon to IFM (black arrows in **a-d, g, h**). Images **a-c** and **e-g** are separate tendon sections. Images **d** and **h** are enlarged images of **c** and **g**, respectively, with correlating blue

and green boxes outlining the enlarged regions. White bars: 500 μm; Red bars: 200 μm; Black bars: 50 μm.

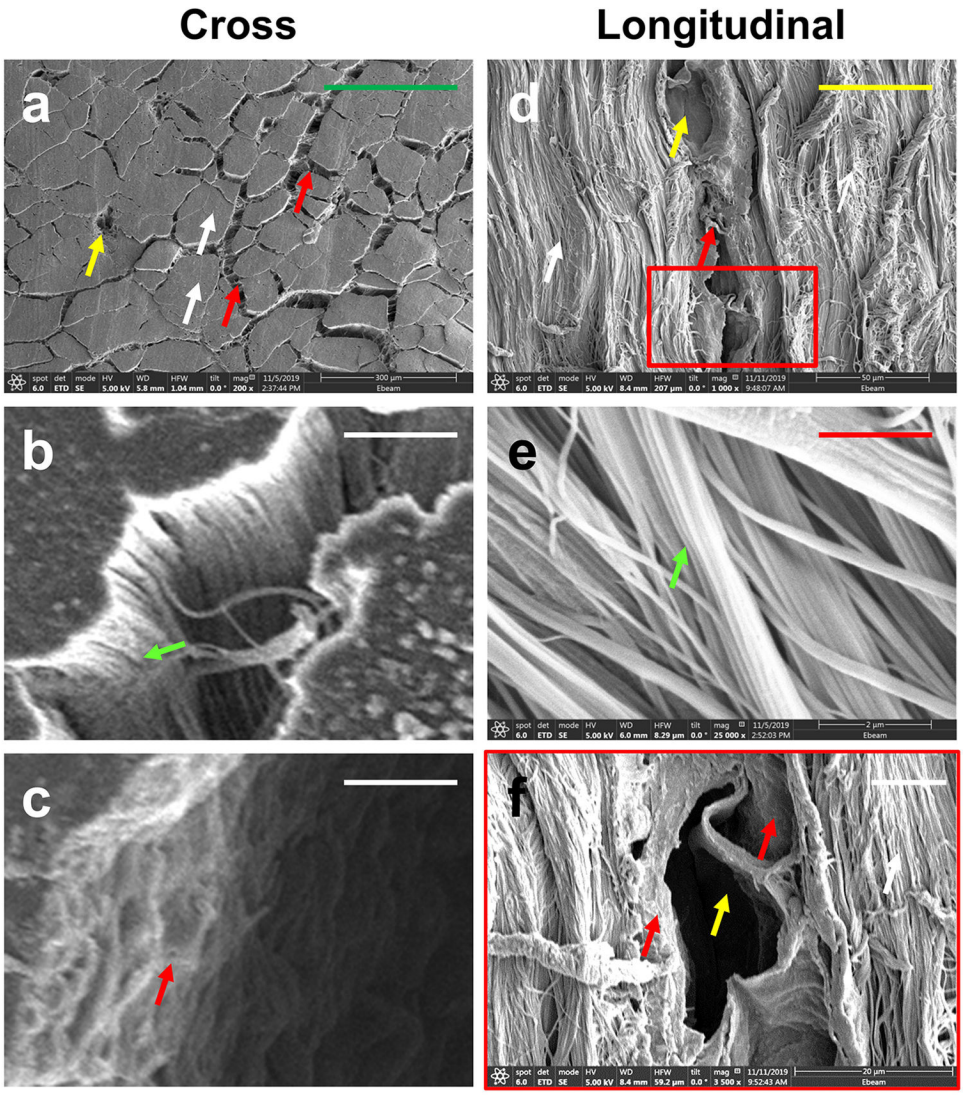

Fig. 4. Scanning electronic microscope (SEM) imaging analysis of PAT.

SEM images of cross and longitudinal sections show a loose net-mesh IFM (red arrows) between the collagen fiber bundles, with the IFM harboring blood vessel-like tissues (yellow arrows in **a, d, f**). The core structure of the tendon (white arrows in **a, d**) is formed by high-density collagen fiber bundles organized into collagen fascicles (green arrows in **b, e**). Overall, the structures of the IFM (red arrow in **c**) and the collagen fascicles (green arrow in **b**) are completely different. The image **f** is the enlarged image of **d**, with a correlating red box. Green bars: 300 μm; Yellow bar: 50 μm; White bars: 10 μm; Red bar: 2 μm.

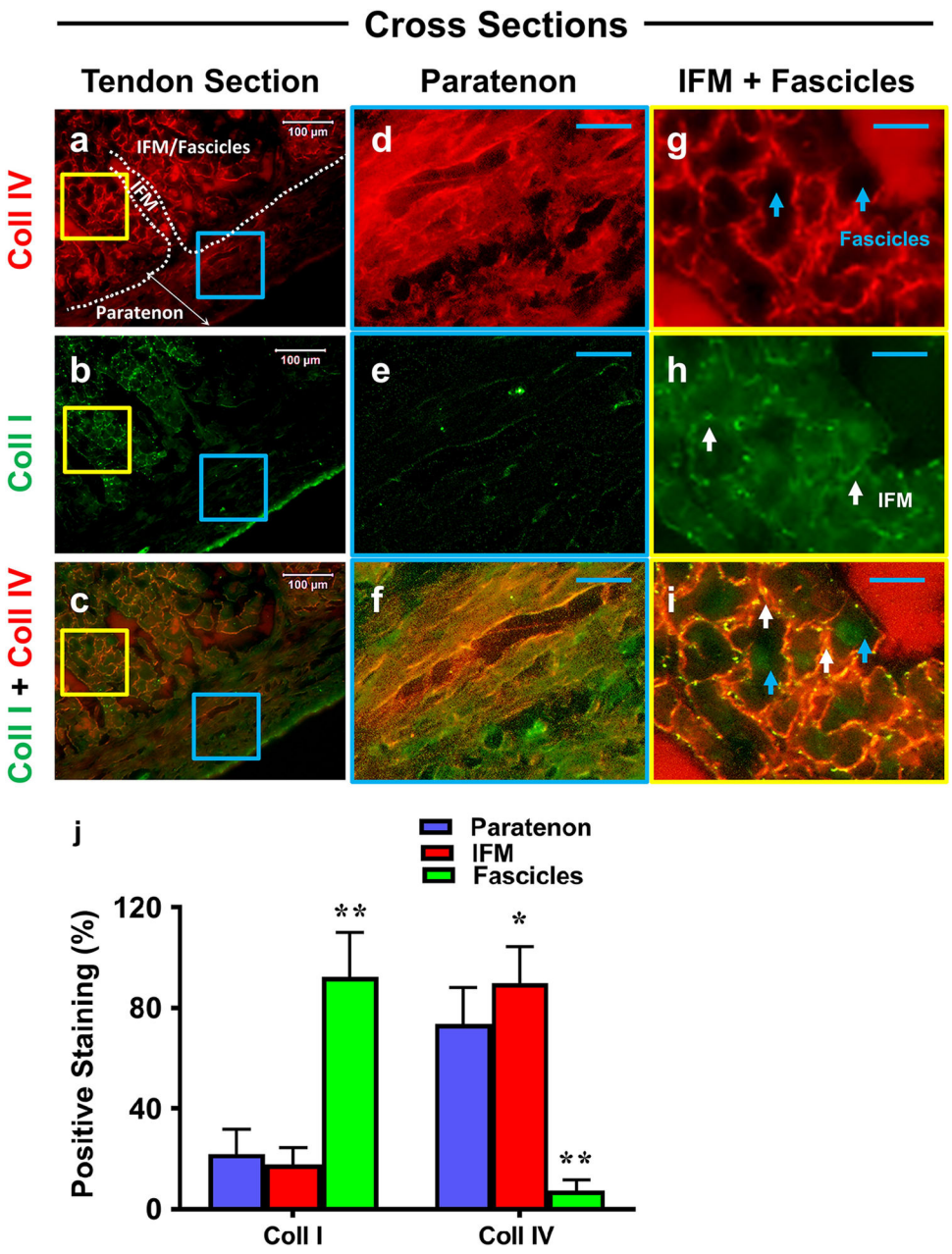

Fig. 5. The differential collagen expression in paratenon, IFM, and fascicles.

Cross-sectional tissue sections were evaluated for collagen I (green fluorescence) and collagen IV (red) expression by immunofluorescent staining. Whole tendon tissue staining in images **a-c**, with enlarged images in blue and yellow boxes in **d-f** and **g-i**, respectively. Images **c**, **f**, and **i** represent merged images. Clear boundaries between the paratenon and IFM/Fascicles are represented within **a** by a white boundary line and appropriate labels. Paratenon tissues are positively stained for collagen IV (**d, f**), and collagen I (**e, f**), albeit its level appears lower than collagen IV. The IFM tissues are positively stained by collagen IV (**g, i**), but produced low levels of collagen I staining (net-like structure, white arrows in **h, i**). Fascicle tissues show strong positive staining by collagen I (**h, i**), but they are negatively

stained by collagen IV (blue arrows in **g, i**). Semi-quantification of these images is displayed in figure **j**. *p < 0.001(IFM compared to paratenon); **p < 0.001 (fascicles compared to paratenon and IFM). White bars: 100 μm; Blue bars: 25 μm.

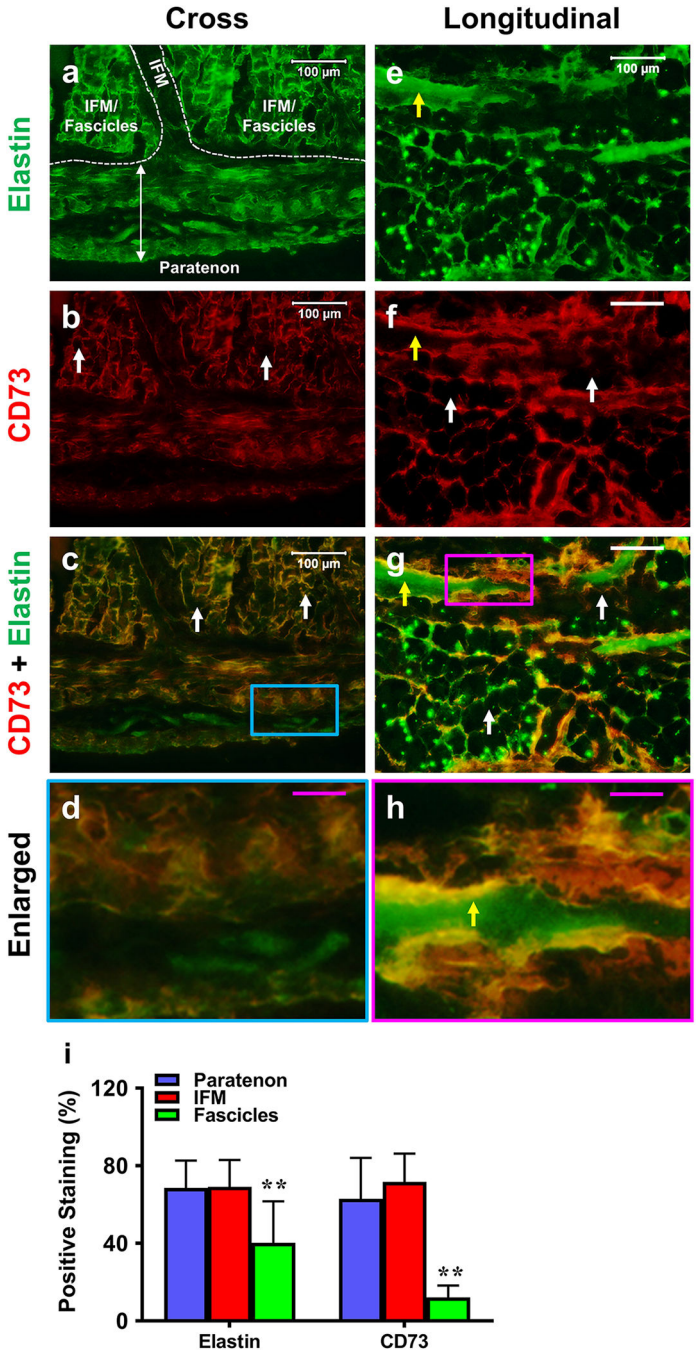

Fig. 6. The differential expression of elastin and CD73 in paratenon, IFM, and fascicles.

Each component is analyzed in cross (**a-d**) and longitudinal sections (**e-h**) staining for elastin (green) and CD73 (red) by immunofluorescent staining. Each component is labeled in **a** with white boundaries designating specific regions of the tendon. Each component is replicated in **a-d** images and in **e-h** images. Paratenon tissues are positively stained with both elastin and CD73 (**a-d**). The interior of blood vessel-like tissues within the IFM are positively stained by elastin (yellow arrow **e, h**), with the exterior positively stained for CD73 (yellow arrows in **f, h**). High levels of net-like IFM are positively stained by elastin

(**a, c, e, g, h**) and CD73 (**b, c, f-h**), whereas fascicles show a minimal amount of staining for elastin and are negative for CD73 (white arrows in **b, c, f, g**). Image **d** is the enlarged blue box area of image **c**. Image **h** is the enlarged pink box area of image **g**. Semi-quantification is displayed in figure **i**. **p < 0.001 (fascicles compared to both paratenon and IFM). Negative staining images were generated for elastin and CD73 antibodies, as described in the methods. Control images did not show any real signal, with only minor background noise (data not shown). White bars: 100 μm; Pink bars: 25 μm.

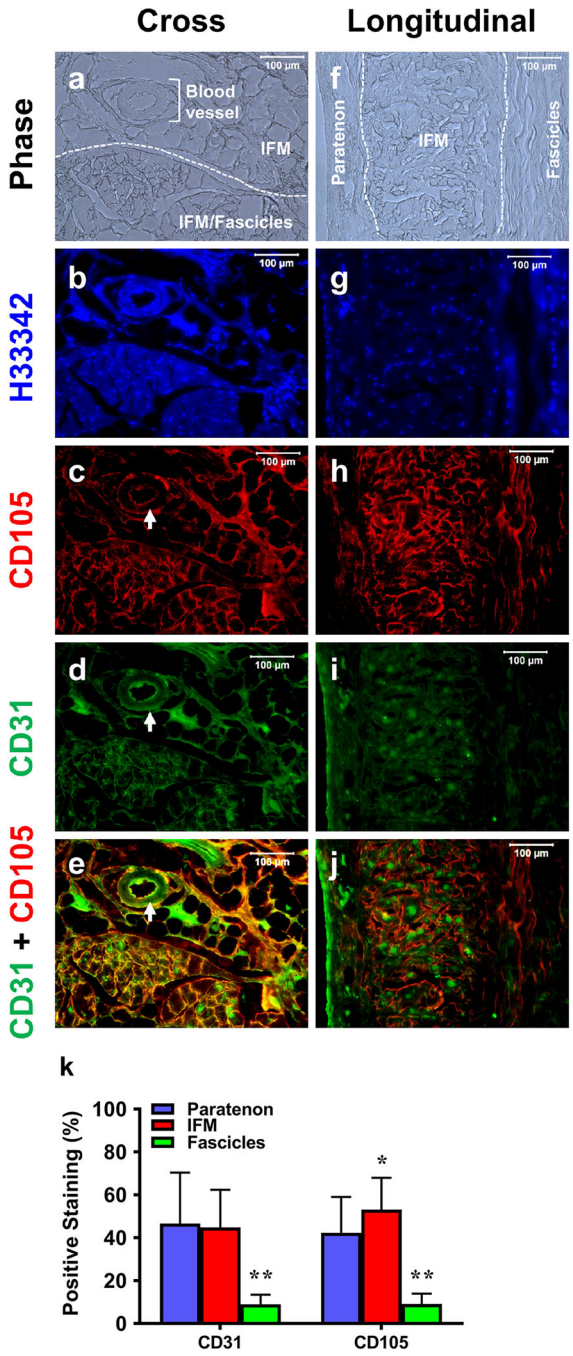

Fig. 7. The differential vascular cell marker expression in paratenon, IFM, and fascicles.

Phase images (**a, f**) and H33342 images (**b, g**) show a clear separation between the paratenon, IFM, and fascicles. Designated and labeled areas in white (**a, f**) are repeated in subsequent images in **a-e** and **f-j**. Images are stained for CD105 (red fluorescence) and CD31 (green fluorescence). Cross sections show that paratenon tissues are positively stained by both CD105 (**c, e**) and CD31 (**d, e**), with blood vessel-like tissues within the IFM positively stained by both CD105 and CD31 on the interior surface (white arrows in **c-e**). High levels of the IFM are positively stained by both CD105 (**c, e**) and CD31 (green in **d, e**),

but fascicles are neither stained by CD105 (empty areas in **c, e**) nor by CD31 (empty areas in **d, e**). Similar results have been found in longitudinal tissue sections (**f-j**). Semi-quantification is displayed in **k**. *$p < 0.05$ (IFM compared to paratenon); **$p < 0.001$ (fascicles compared to paratenon and IFM). White bars: 100 μm.

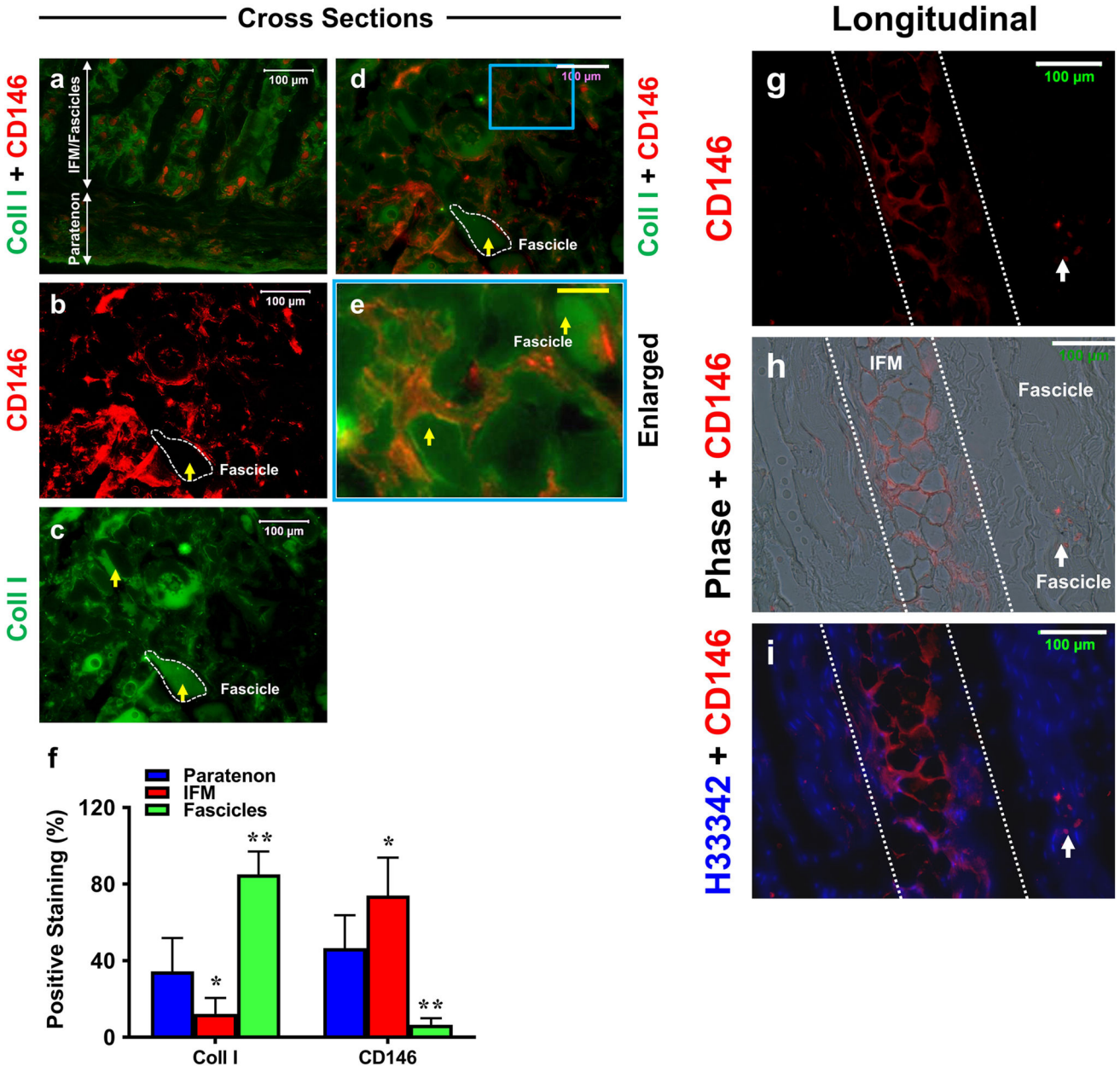

Fig. 8. The differential CD146 and collagen type I expression in tendon tissue sections.

Cross (**a-e**) and longitudinal (**g-i**) tissue sections are stained for CD146 (red fluorescence) and collagen I (green fluorescence), compared to Hoechst H33342 staining (**h**) and phase contrast images (**h**). Cross sections show paratenon tissues are positively stained for both CD146 (**a**) and collagen I (**a)**, IFM also is stained for CD146 and collagen I (**a-e**), and fascicles are positive for collagen I (**a, c-e**). Semi-quantification of **a-e** is displayed in **f**. *$p < 0.001$ (IFM compared to paratenon); **$p < 0.001$ (fascicles compared to both paratenon and IFM). Additional longitudinal tissue sections (**g-i**) show the IFM (the areas between white dash lines) positively stained for CD146, but very few cells in fascicles are positively stained by CD146 (white arrows). Thus, fascicles are only positively stained by collagen I (yellow arrows in **b-e**). The image **e** is the enlarged blue box area within image **d** which shows that

IFM tissues are stained positively by CD146 and fascicles are positively stained by collagen I. White bars: 100 μm; Yellow bar: 25 μm.

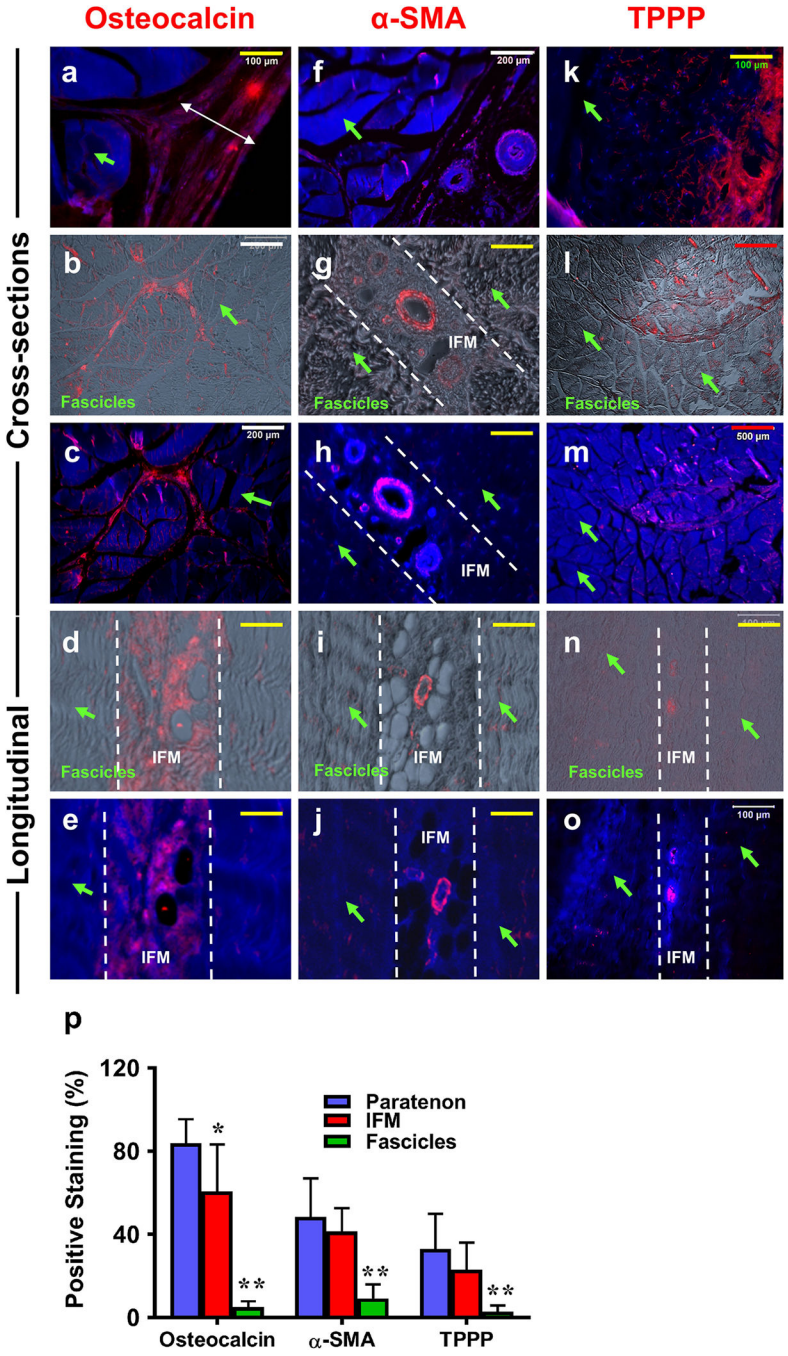

Fig. 9. Osteocalcin, alpha-smooth muscle actin (α-SMA), and tubulin polymerization promoting protein (TPPP) expression on PAT tissue sections determined by immunostaining.

a-e: Osteocalcin staining; **f-j:** α-SMA staining; **k-o**: TPPP staining. Cross and longitudinal sections are labeled on the left of the image. **a, c, e**: The cells were stained with H33342 (blue) and osteocalcin (red); **f, h, j:** The cells were stained with H33342 (blue) and α-SMA (red); **k, m, o**: The cells were stained with H33342 (blue) and TPPP (red); **b, d**: Merged images of osteocalcin (red) and phase contrast images; **g, i:** Merged images of α-SMA(red) and phase contrast images. **l, n**: Merged images of TPPP (red) and phase contrast images.

The results showed that the paratenon (**a**) and IFM (**b-e**) are positively stained for osteocalcin, but fascicles are negatively stained by osteocalcin (green arrows in **a-e**). The blood vessel-like tissues within the paratenon (**f**) and IFM (**g-j**) are specifically stained for α-SMA, but both overall IFM and fascicles are negatively stained by α-SMA (white lines demarcating the IFM, green arrows for fascicles in **f-j**). Paratenon tissues are positively stained by TPPP (red fluorescence in **k**), while a low amount of staining can be seen within IFM tissues (red fluorescence in **l-o**). No fascicles are positively stained for TPPP (green arrows **k-o**). Semi-quantification is displayed in figure **p,** *$p < 0.001$ (IFM compared to paratenon); **$p < 0.001$ (fascicles compared to both paratenon and IFM). White bars: 200 μm; Yellow bars: 100 μm; red bars: 500 μm.

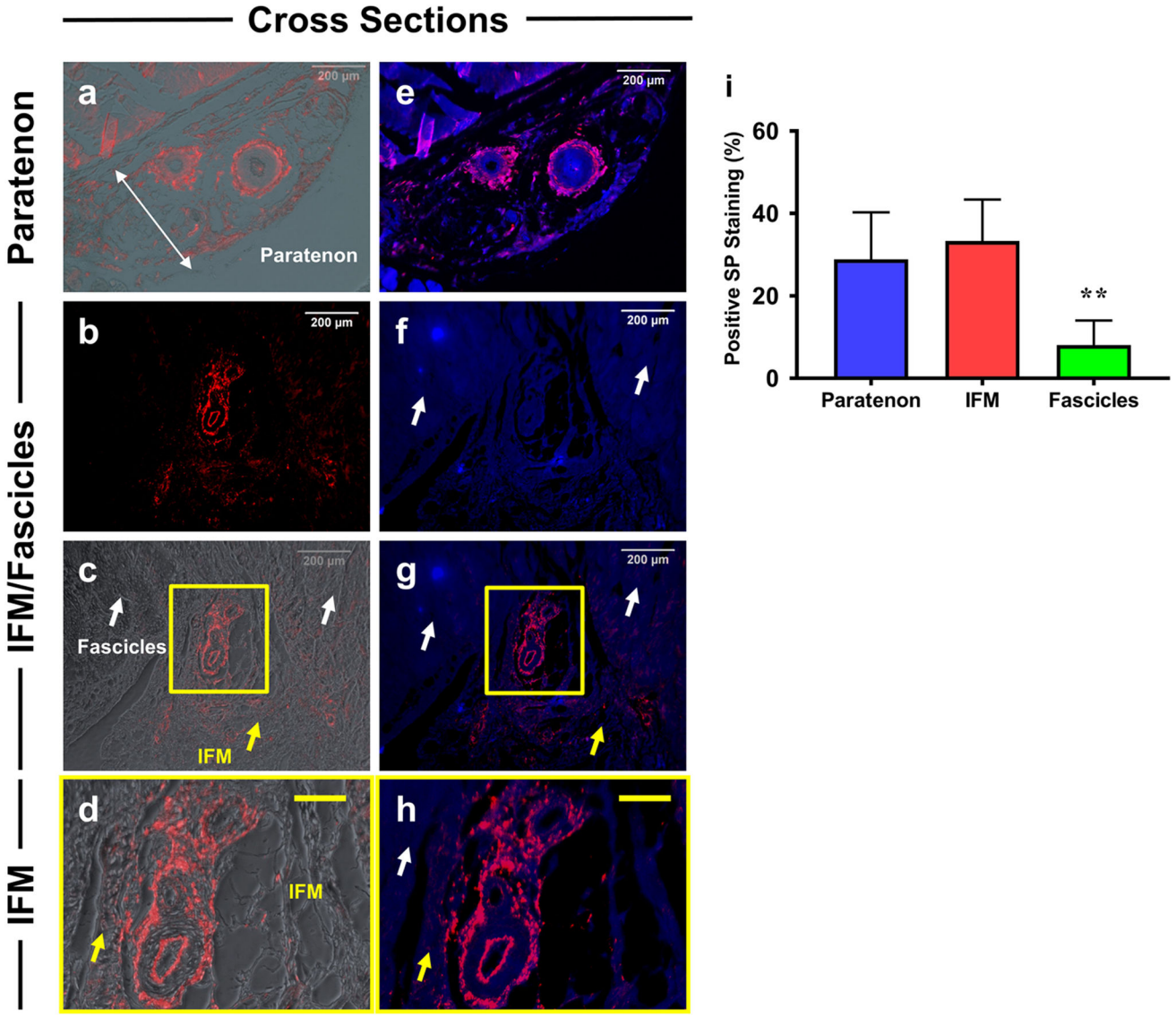

Fig. 10. Differential expression of Substance P (SP) in paratenon, IFM, and fascicles.

a, c, d: Merged images of positively staining on SP (red) and phase contrast images. **b**: Tissue stained for substance P only. **e, g, h**: Merged images of SP (Red) and H33342 (blue). **f**: H33342 (blue) staining only. Results show that only blood vessel-like tissues in paratenon (**a, e**) and IFM (**b, c, g**) are positively stained by SP (red fluorescence), but fascicles (white arrows in **b, c, f, g, h**) and overall IFM tissues (yellow arrows in **c, d, g, h**) are negatively stained by SP. Semi-quantification is displayed in figure **i**. **p < 0.001 (fascicles compared to paratenon and IFM). White bars: 200 μm; Yellow bars: 50 μm.

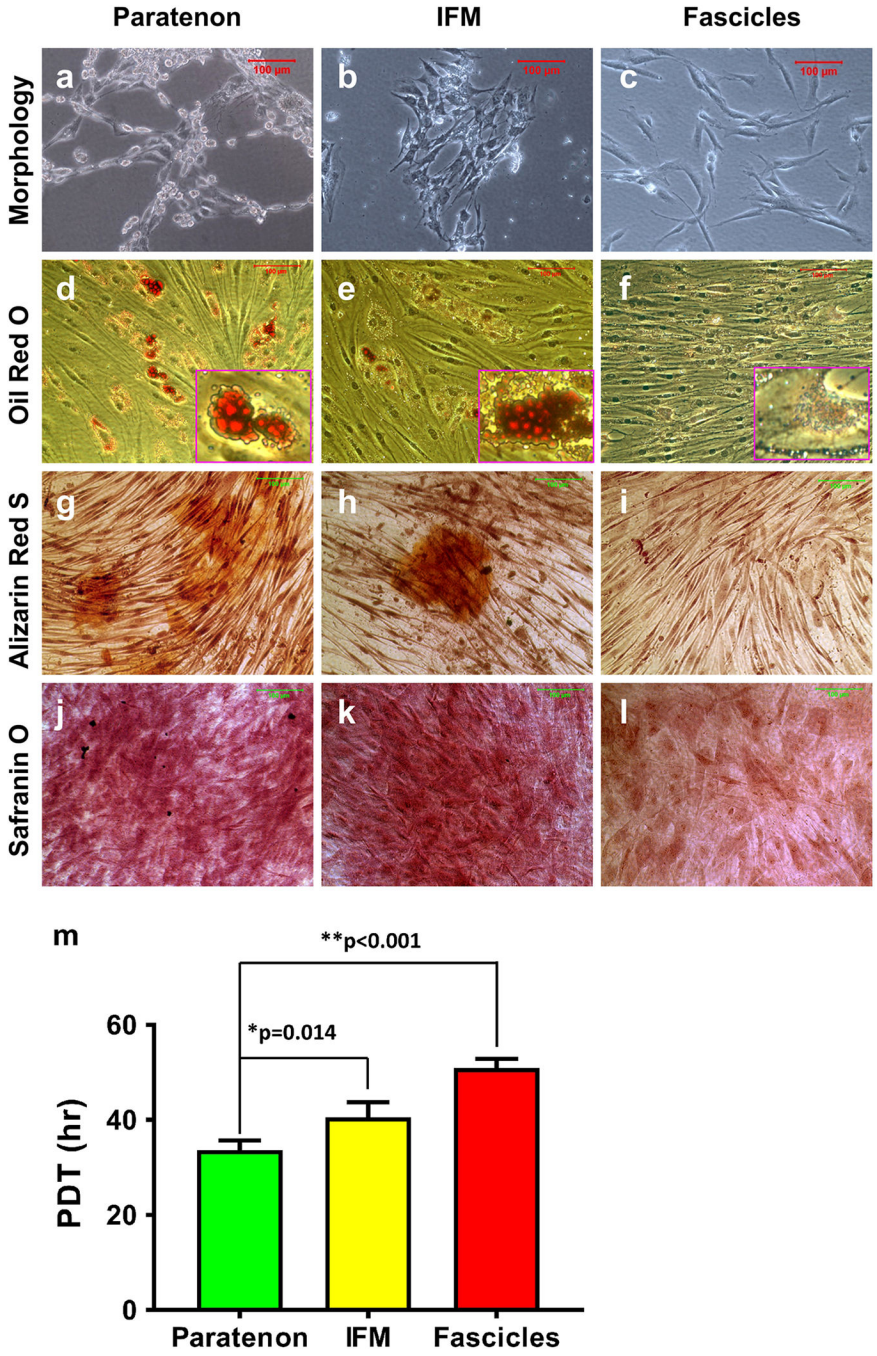

Fig. 11. Differential morphologies and population doubling time of *in vitro* isolated cells from paratenon, IFM, and fascicles.

Cells were harvested and analyzed for morphology at day 8 during primary culture. Phase contrast images of cells from the paratenon (**a**), IFM (**b**), and fascicles (**c**) were collected and analyzed. Isolated paratenon cells were endothelial-like, IFM isolated cells exhibited cobblestone-like morphology suggestive of stem cells, and isolated fascicle cells exhibited an elongated fibroblast-like morphology. Each cell population was assessed for multi-differentiation potential, with oil red O staining (**d-f**) assessing for adipogenesis, alizarin

Red S staining (**g-i**) testing for osteogenesis, and safranin O staining (**j-l**) for chondrogenesis. The population doubling time (PDT) indicates that cells isolated from the paratenon grew faster than cells isolated from IFM and fascicles. Quantification of PDT is displayed in figure **m**, with resulting p values: *$p = 0.014$ (IFM compared to paratenon), and **$p < 0.001$ (fascicles compared to paratenon and IFM). Red bars: 100 μm.

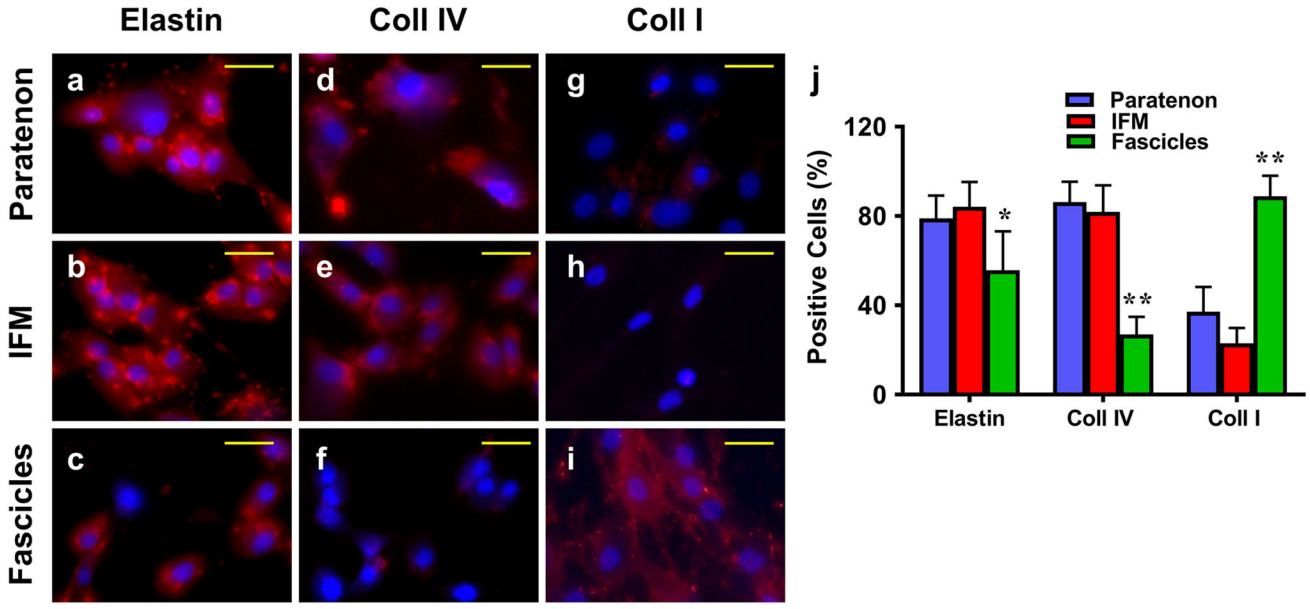

Fig. 12. Immunostaining of isolated cells from paratenon, IFM, and fascicles for expression of structural tendon proteins.

Passage 2 cells were analyzed with ICC. **a-c**: Elastin; **d-f**: Collagen IV; **g-i**: Collagen I; **a, d, g**: paratenon isolated cells; **b, e, h**: IFM isolated cells; and **c, f, i**: Fascicle isolated cells. All components expressed elastin, with high levels in the paratenon and IFM isolated cells (**a, b**), and minimal levels within fascicle isolated cells (**c**). High levels of collagen IV staining can be seen in both the paratenon and IFM (**d, e**), with very few positively stained cells within fascicle isolated cultures (**f**). Collagen I is apparently expressed at a low level in isolated paratenon (**g**) and is minimally expressed in IFM (**h**) cell cultures, while isolated fascicle cells presented high levels of expression for collagen I. (**i**). Semi-quantification is displayed in figure **j**, *$p < 0.01$ (fascicles compared to IFM); **$p < 0.001$ (fascicles compared to both paratenon and IFM). Yellow bars: 25 μm.

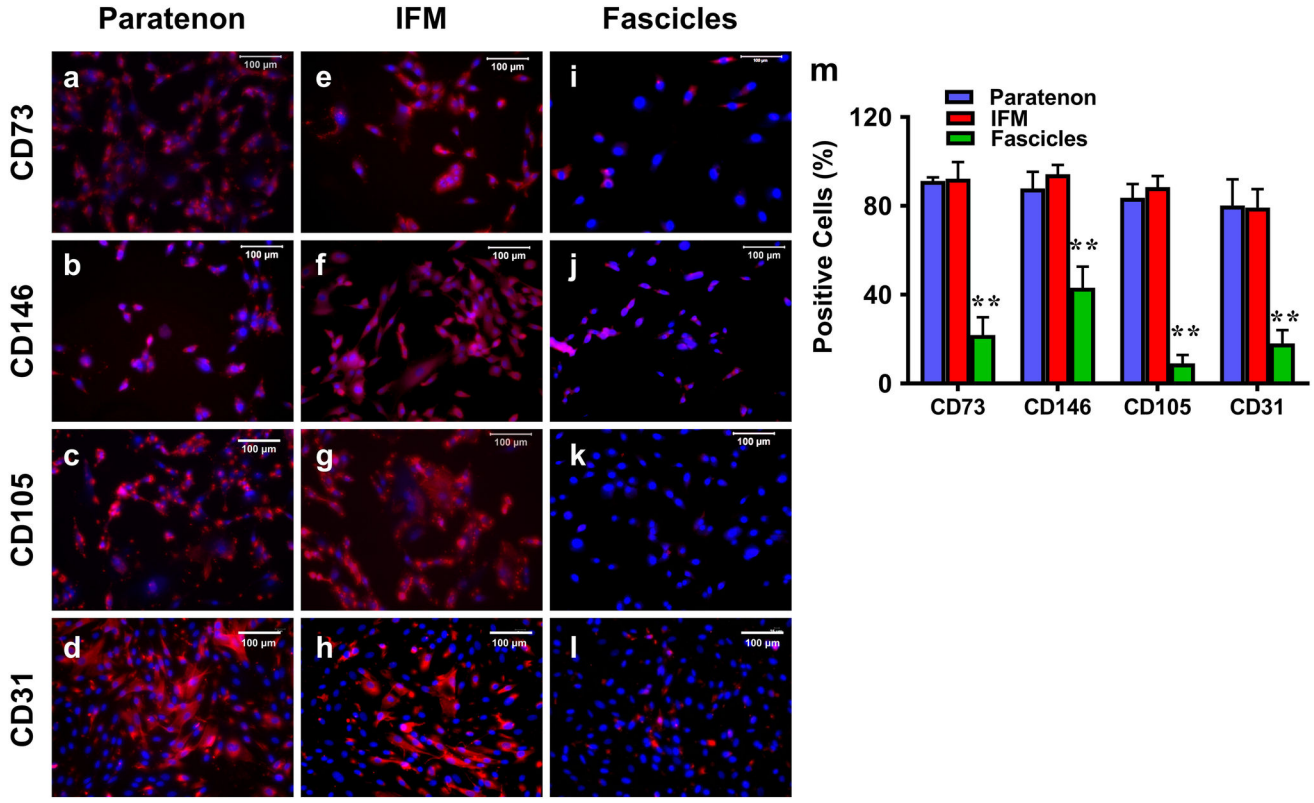

Fig. 13. Immunostaining of isolated cells from paratenon, IFM, fascicles *in vitro* for expression of stem cell and vascular markers.

a-d: paratenon isolated cells; **e-h**: IFM isolated cells; **i-l**: fascicle isolated cells; **a, e, i**: CD73 staining; **b, f, j**: CD146 staining; **c, g, k**: CD105 staining; and **d, h, l**: CD31 staining. Cells isolated from the paratenon and IFM expressed markers CD73, CD146, CD105, and CD31 (**a-d, e-h**), while fascicle isolated cells only expressed CD73, CD146, and CD31 at minimal levels, and exhibited no expression of CD105 (**i-l**). Semi-quantification is displayed in figure **m,** **$p < 0.001$ (fascicles compared to both paratenon and IFM). White bars: 100 µm.

Table 1

Summary of PAT Structure

	Paratenon	IFM	Fascicle
Tendon structure	**Loose sheath**	**Loose net-like mesh structure**	**Densely packed fiber bundles**
Collagen I	minimal	minimal	+
Collagen IV	+	+	--
Elastin	+	+	minimal
CD73	+	+	--
CD105	+	+	--
CD31	+	+	--
CD146	+	+	minimal
Osteocalcin	+	+	--
α-SMA	+ at BVs	+ at BVs	--
TPPP	+	minimal	--
Substance P	+ at BVs	+ at BVs	--

PAT = porcine Achilles tendon; + = Positive staining; BVs = blood vessels

Table 2

Summary of PAT Cells in Culture

	Paratenon	IFM	Fascicle
Tendon cell morphology	**Endothelial-like cells**	**Cobblestone-like; with many colonies, highly proliferative**	**Elongated fibroblast-like tenocytes; no colonies**
PDT	33.6 hrs	40.5 hrs	50.9 hrs
Collagen I	--	--	+
Collagen IV	+	+	--
Elastin	+	+	minimal
CD73	+	+	minimal
CD105	+	+	--
CD31	+	+	--
CD146	+	+	minimal

PAT = porcine Achilles tendon; + = Positive staining; PDT = population doubling time as reported in Fig. 11d.